Research Resource: Monitoring Endoplasmic Reticulum Membrane Integrity in β-Cells at the Single-Cell Level

Kohsuke Kanekura, Jianhong Ou, Takashi Hara, Lihua J. Zhu, and Fumihiko Urano

Department of Medicine (K.K., T.H., F.U.), Division of Endocrinology, Metabolism, and Lipid Research, and Department of Pathology and Immunology (F.U.), Washington University School of Medicine, St Louis, Missouri 63110; and Programs in Gene Function and Expression, Molecular Medicine, and Bioinformatics and Integrative Biology (J.O., L.J.Z.), University of Massachusetts Medical School, Worcester, Massachusetts 01655

Endoplasmic reticulum (ER) membrane integrity is an emerging target for human chronic diseases associated with ER stress. Despite the underlying importance of compromised ER membrane integrity in disease states, the entire process leading to ER membrane permeabilization and cell death is still not clear due to technical limitations. Here we describe a novel method for monitoring ER membrane integrity at the single-cell level in real time. Using a β-cell line expressing ER-targeted redox sensitive green fluorescent protein, we could identify a β-cell population undergoing ER membrane permeabilization induced by palmitate and could monitor cell fate and ER stress of these cells at the single-cell level. Our method could be used to develop a novel therapeutic modality targeting the ER membrane for ER-associated disorders, including β-cell death in diabetes, neurodegeneration, and Wolfram syndrome. (*Molecular Endocrinology* 29: 473–480, 2015)

Type 2 diabetes is defined by hyperglycemia caused by a relative deficiency of insulin. It has been proposed that β-cell death is an important pathogenic component of type 2 diabetes (1–3). Type 2 diabetes is the most common form of diabetes and is associated with obesity and hyperlipidemia. It has been established that prolonged exposure to elevated fatty acids causes impaired glucose-stimulated insulin secretion, suppression of insulin gene expression, and apoptosis of β-cells. Multiple models have been proposed to explain the underlying mechanisms by which elevated free fatty acids trigger dysfunction and death of β-cells (4–12).

Endoplasmic reticulum (ER) plays a range of vital roles including synthesis and oxidative folding of secretory proteins, calcium homeostasis, and regulation of cell death. Dysregulation of ER homeostasis activates the unfolded protein response, which controls the cell fate either to adapt to stress or to initiate apoptosis (13). Recently it has been shown that saturated fatty acids target the ER and trigger ER stress in β-cells (4, 5, 12, 14). The lipid profile of ER membrane and ER morphology are also affected by overloading of free fatty acids, and palmitate, a saturated fatty acid, induces the disruption of ER membrane integrity (15). Impairment of the integrity of ER membrane followed by the leakage of ER contents, including calcium, has been shown under various chemical or pathological ER stress conditions (15–18). Although the leakage of ER contents possibly contributes to malfunction of ER and initiation of apoptosis, the underlying mechanisms have been poorly investigated due to the lack

ISSN Print 0888-8809 ISSN Online 1944-9917
Printed in U.S.A.

Received August 17, 2014. Accepted January 9, 2015.
First Published Online January 13, 2015

Abbreviations: AICAR, 5-aminoimidazole-4-carboxamide ribonucleotide; Bak, Bcl-2-antagonist/killer; Bax, Bcl-2-associated X protein; BiP, immunoglobulin heavy chain-binding protein; Chop, CCAAT/enhancer-binding protein homologous protein; ER, endoplasmic reticulum; FBS, fetal bovine serum; GFP, green fluorescent protein; MEF, mouse embryonic fibroblast; PA, palmitic acid; PI, propidium iodide; Puma, p53 up-regulated modulator of apoptosis; roGFP, redox-sensitive GFP; wt-MEF, wild-type MEF; XBP1, X-box binding protein.

of methods for detecting the loss of integrity of the ER membrane. Here we report a novel method for evaluating the ER membrane integrity in palmitate-treated β-cells at the single-cell level.

Materials and Methods

Reagents

Palmitate, oleate, linoleate, tunicamycin, and 5-aminoimidazole-4-carboxamide ribonucleotide (AICAR) were obtained from Sigma-Aldrich. Antiglucose-regulated protein-94 antibody, anticalreticulin antibody, anti-green fluorescent protein (GFP) antibody, and antiglyceraldehyde-3-phosphate dehydrogenase antibody were obtained from Cell Signaling Technology. Antivesicle-associated membrane protein-associated protein B antibody was obtained from Bethyl. RPMI 1640, DMEM, and propidium iodide (PI) solution were obtained from Invitrogen.

Cell culture

INS-1 832/13 cells were cultured in the RPMI 1640 supplemented with 10% fetal bovine serum (FBS), penicillin and streptomycin, sodium pyruvate, and 0.1% β-mercaptoethanol. Mouse embryonic fibroblasts were cultured in DMEM containing 10% FBS and antibiotics. Primary humans islets, obtained from Prodo, were plated onto a six-well plate (1500 islets/well) precoated with laminin V produced by 804G cells and cultured in CMRL medium (medium developed at the Connaugh Medical Research Laboratories) supplemented with FBS, nonessential amino acids, sodium pyruvate, and antibiotics. For establishing stable cell lines, cells were transduced with lentiviruses expressing MERO-GFP (pLenti-CMV-puro-MERO-GFP) and selected with puromycin. The lentivirus vectors including pLenti-CMV-puro-dest vector was obtained from Addgene.

Preparation of fatty acids

Palmitate, oleate, and linoleate were conjugated with BSA by soaping each fatty acid to sodium hydroxide and mixing with BSA as described previously (19). Twenty millimolar of the solution of each fatty acid in 0.02 M NaOH was incubated at 70°C for 30 minutes and then mixed with 5% BSA in PBS in a 1:3 vol ratio. Each solution was diluted with 10% FBS-RPMI 1640 medium to the designated concentration.

Fluorescence-activated cell sorter (FACS) analyses

For flow cytometry analyses, INS-1 832/13 and mouse embryonic fibroblasts (MEFs) expressing MERO-GFP or cytosolic redox-sensitive GFP (roGFP) were plated onto 12-well plates, treated with each compound for the indicated times, and then harvested by trypsinization. Flowcytometry analyses were performed with LSRII (BD Biosciences). The results were analyzed by FlowJo version 7.6.3 (TreeStar).

Quantitative real-time PCR

INS1-MERO-GFP cells treated with 0.5 mM palmitic acid (PA) were sorted by FACS AriaIII (BD Biosciences) according to the ratio of MERO-GFP. Total RNA was extracted by RNeasy kits (QIAGEN). RT-PCRs were performed using ImPromII (Promega) reverse transcriptase, and quantitative real-time PCR was performed with Biorad iQ5 using SYBR green dye (Bio-Rad Laboratories). The primers used in the assays are the followings: for rat β-actin, GCAAATGCTTCTAGGCGGAC and AAGAAAGGGTGTAAAACGCAGC; for rat immunoglobulin heavy chain-binding protein (BiP), TGGGTACATTTGATCTGACTGGA and CTCAAAGGTGACTTCAATCTGGG; for rat spliced X-box binding protein (XBP1), CTGAGTCCGAATCAGGTGCAG and ATCCATGGGAAGATGTTCTGG; for rat CCAAT/enhancer-binding protein homologous protein (Chop), AGAGTGGTCAGTGCGCAGC and CTCATTCTCCTGCTCCTTCTCC; and for rat p53 up-regulated modulator of apoptosis (Puma), GCGGAGACAAGAAGAGCAAC and CTCCAGGATCCCTGGGTAAG.

Gene expression profiling

INS1-MERO-GFP cells treated with 0.5 mM PA for 24 hours were sorted by FACS-AriaIII (BD Biosciences), and total RNA was extracted with a RNeasy kit (QIAGEN). The purified RNA was applied to a GeneChip Rat Gene 1.0 ST array (Affymetrix) according to the manufacturer's protocols. The obtained data were analyzed by getting the difference from each pair of cells with the MERO to GFP ratio greater than 2 and less than 2, and we set the value of the mean of each pair as 0. The heat map was generated from the data reflecting the differences of gene expressions in each pair in log2 scale.

Transmission electron microscopy

INS-1 832/13 cells and human primary islets plated onto a six-well plate were fixed by adding 1 mL of 2.5% glutaraldehyde (vol/vol) in 0.1 M Na cacodylate-HCl buffer (pH 7.2) to each of the wells containing 1 mL of media. The cells were then fully fixed with 2.5% glutaraldehyde (vol/vol) in 0.1 M Na cacodylate-HCl buffer (pH 7.2) overnight at 4°C. The fixed samples, washed three times in 0.1 M Na cacodylate-HCl buffer (pH 7.2), were pelleted and postfixed for 1 hour in 1% osmium tetroxide (wt/vol) in distilled water. The fixed cells, dehydrated through a series of ethanol, were transferred through two changes of propylene oxide and then into a mixture of 50% propylene oxide/50% epon resin. The epoxy blocks were trimmed, and ultrathin sections of 70 nm were cut on a Reichart-Jung ultramicrotome. The sections, contrasted with lead citrate and uranyl acetate, were examined using a FEI Tecani 12 BT with 80-Kv accelerating voltage, and images were captured using a Gatan transmission electron microscopy charge-coupled device camera.

Live imaging

INS1-MERO-GFP cells were plated on a poly-L-lysine-coated, glass-bottom, 35-mm dish (MatTek) the day before the analysis. The cells were then cultured with 10% FBS-RPMI 1640 medium containing 0.4 mM PA and 0.5 μg/mL of PI in 5% CO_2 at 37°C for 15 hours. The images were captured every 20 minutes using a Yokogawa spinning disk confocal on a Nikon TE-2000E2 inverted microscope with a ×40 objective lens. All analyses were done on 16-bit or 32-bit images using ImageJ 1.45 (National Institutes of Health, Bethesda, Maryland).

Cell fractionation

The fractionation of cytosol and membranous organelles from INS1 832/13 cells treated with or without PA were done by a Qproteome cell compartment kit (QIAGEN) following the manufacture's protocol. After fractionation, an equal volume of the lysates was subjected to SDS-PAGE followed by immunoblot analyses.

Mass spectrometry and liquid chromatography and mass spectrometry analysis

Liquid chromatography and mass spectrometry analysis of lipid was conducted on a Thermo Scientific Vantage TSQ mass spectrometer with Thermo Accela UPLC operated by Xcalibur software. Mass spectra of the eluted peaks containing the phospholipids in the same family were averaged, and the lipid profiles among samples were compared. Structural identification of the lipid species was performed on a Thermo Scientific LTQ Orbitrap Velos mass spectrometer with an Xcalibur operating system.

Results

Palmitate alters lipid composition of the ER membrane and disrupts its structure

To test whether palmitate alters the lipid composition of the ER membrane in pancreatic β-cells, ER fractions from a rat insulinoma cell line, INS1 832/13 cells, treated with 0.5 mM plamitate or 0.5 mM oleate for 24 hours were analyzed with liquid chromatography-mass spectrometry (Figure 1A). Both palmitate and oleate increased the quantity of lipid species in the ER membrane (20). The degree of saturation of fatty acids was also increased by treatment with palmitate (Supplemental Figure 1).

It has been shown that increased saturation of lipid species in biological membrane is associated with stiffness and less flexibility of membrane (21–23). To test whether palmitate damages ER membrane structure in β-cells, we treated INS1 832/13 cells and human primary islets with palmitate. To minimize the effects of apoptosis on the membrane structure, we treated INS1 832/13 cells and human primary islets with 0.5 mM palmitate for 4 hours and then examined the morphology of the ER using transmission electron microscopy. In untreated cells, the morphology of the ER appeared normal (Figure 1, B–E), whereas palmitate-treated cells showed dilated ER with discontinuous ER membrane and dissociation of ribosomes from the rough ER (Figure 1, F–I). Furthermore, treatment with palmitate induced the mislocalization of ER-DsRed, a red fluorescent protein expressed in the lumen of the ER, in human embryonic kidney-293 cells (Supplemental Figure 2). Collectively these results indicate that palmitate directly impairs the ER membrane integrity and induces ER stress in β-cells (5, 15, 24, 25).

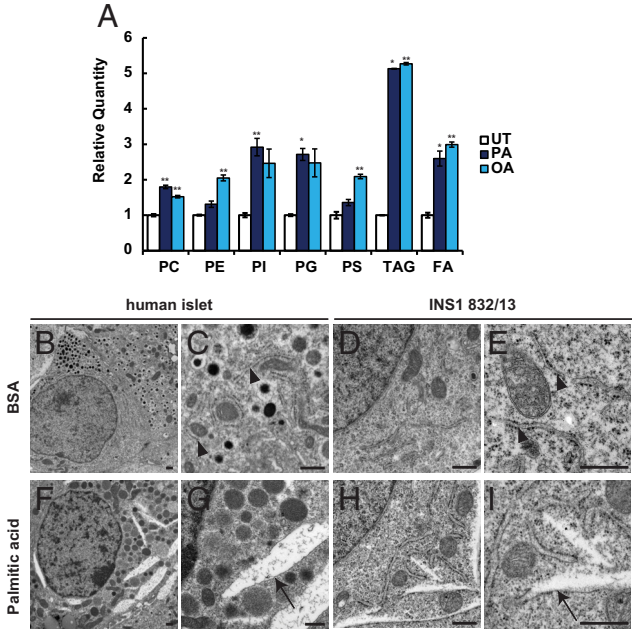

Figure 1. A, Relative quantity of lipid species in the ER fractions of INS1 832/13 cells treated with 0.5 mM PA or 0.5 mM oleic acid (OA) or untreated (UT) (n = 3.). PC, phosphatidylcholine; PE, phosphatidylethanolamine; PI, phosphatidylinositol; PG, phosphatidylglycerol; PS, phosphatidylserine; TAG, triacylglycerol; FA, fatty acid. Error bars show SE. *, $P < .05$; **, $P < .01$. B–I, Transmission electron microscope images of human islet or INS1 832/13 cells treated with BSA (control) or 0.5 mM PA. B and C, Human islet treated with BSA. D and E, INS1 832/13 cells treated with BSA. F and G, Human islet treated with PA. H and I, INS1 832/13 cells treated with PA. Arrowheads and arrow indicate normal ER and disrupted ER, respectively.

Disruption of ER membrane by palmitate causes the leakage of ER contents to the cytosol in cardiomyocytes and pancreatic β-cells (15, 17, 26). To date, the evaluation of the leakage of ER contents depends on cell fractionation of bulk-prepared cells and tissues, followed by immunoblot, and it has been difficult to analyze at the single-cell level. To overcome this challenge, we adopted the roGFP localizing to mammalian ER (mammalian ER localized roGFP, MERO-GFP) (25, 27, 28). We have previously shown that MERO-GFP is specifically localized to the ER (28). Depending on the status of an artificially inserted cysteine pair, roGFP can indicate precise redox change by calculating the ratio of the signal from excitation at 488 nm and signal from excitation at 405 nm (Figure 2A). Because the ER lumen has a highly oxidative environment, the ratio between reduced and oxidized roGFP expressed in the ER (MERO-GFP ratio) is much lower than the ratio between reduced and oxidize roGFP expressed in the cytosol (cytosolic roGFP ratio) (Figure 2B) (28). We therefore considered the possibility that the dramatic shift of the roGFP ratio can be used to detect the leakage of MERO-GFP to the cytosol (Figure 2, B and C). To test this, INS1 832/13 cells stably expressing MERO-

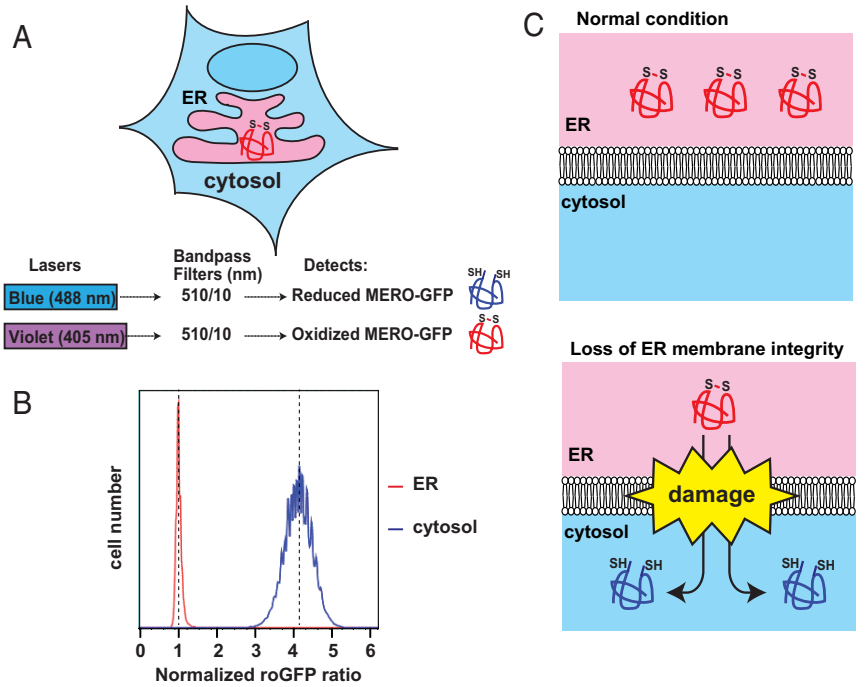

Figure 2. A, Scheme of setting of a flow cytometer for detection of MERO-GFP. B, Histogram of INS1 832/13 cells expressing MERO-GFP (red) or cytosolic roGFP (blue). Dashed lines indicate the median or MERO-GFP and cytosolic roGFP. The ratio of roGFP is normalized to the MERO-GFP ratio. C, Scheme of translocation of MERO-GFP from oxidative ER to reduced cytosol. Each experiment was repeated at least three times independently. -S-S-, a disulfide bone between two cysteines; -SH, a free thiol of cysteine.

GFP (INS1-MERO-GFP cells) were treated with BSA, 0.5 mM palmitate, 0.5 mM oleate, or 0.5 mM linoleate for 16 hours, and the MERO-GFP ratio was determined by flow cytometry. Palmitate but not oleate or linoleate created a cell population harboring an MERO-GFP ratio greater than 2, indicating that MERO-GFP leaked to the cytosol in this population (Figure 3, A–C). Interestingly, the combination of palmitate and oleate or linoleate did not create the cell population harboring MERO-GFP ratio greater than 2, raising the possibility that oleate and linoleate may prevent the disruption of ER membrane by palmitate (Figure 3C). To test this idea, we treated the INS1 832/13 cells with BSA, 0.5 mM palmitate, or 0.5 mM palmitate in combination with 0.5 mM oleate or 0.5 mM linoleate for 16 hours and then performed cell fractionation analysis (Figure 3D). Consistent with the observations from the flow cytometry analysis, both oleate and linoleate prevented the leakage of ER luminal proteins to the cytosol mediated by palmitate. Collectively these findings indicate that oleate and linoleate can prevent the disruption of ER membrane by palmitate

Bcl-2 family proteins, Bcl-2-associated X protein (Bax) and Bcl-2-antagonist/killer (Bak), have been reported to play a role in the ER membrane permeabilization under ER stress conditions, raising the possibility that palmitate-induced ER membrane disruption might be mediated by Bax and Bak (16). To test this idea, wild-type MEFs (wt-MEFs) or Bax/Bak double-knockout MEFs stably expressing MERO-GFP were treated with BSA, 0.2 mM palmitate, or 0.5 mM palmitate. To minimize the effects of apoptosis on the membrane integrity, we treated wt-MEFs and double-knockout MEFs for 6 hours, which did not induce apparent cell death, and then monitored MERO-GFP distribution to the cytosol by flow cytometry. We found that deletion of Bax/Bak did not prevent the creation of a cell population harboring MERO-GFP ratio greater than 2 (Supplemental Figure 3A). Cell fractionation followed by immunoblot assay showed that deletion of Bax/Bak prevented the leakage of ER luminal proteins to the cytosol mediated by a canonical ER stress inducer, tunicamycin, but not by palmitate, suggesting that palmitate-induced ER membrane disruption is not Bax/Bak dependent (Supplemental Figure 3B). AICAR, an activator for AMP-dependent protein kinase, has been reported to confer protection against palmitate-mediated cell death (29, 30). We were therefore interested in determining whether AICAR could prevent the ER membrane permeabilization by palmitate. We treated INS1-MERO-GFP cells with 0.25 mM palmitate in combination with or without 0.5 mM AICAR for 1 hour and analyzed the distribution of MERO-GFP with flowcytometry. As expected, AICAR significantly decreased the creation of a cell population harboring the MERO-GFP ratio greater than 2 (Supplemental Figure 3C).

Loss of ER membrane integrity destroys the oxidative environment in the ER lumen. We have previously reported that palmitate treatment depletes ER calcium store, which impairs the functions of calcium-dependent chaperones localized to ER, resulting in ER stress (31). Therefore, it is possible that the cells experiencing the loss of ER membrane integrity have higher ER stress levels due to the inefficient protein folding. To test this possibility, INS1-MERO-GFP cells were treated with 0.5 mM palmitate and then sorted by flow cytometry based on MERO-GFP ratio (Figure 4A). Gene expression profiles of sorted cells showed that genes involved in ER stress were upregulated in a cell population harboring an MERO-GFP ratio greater than 2 as compared with a cell population

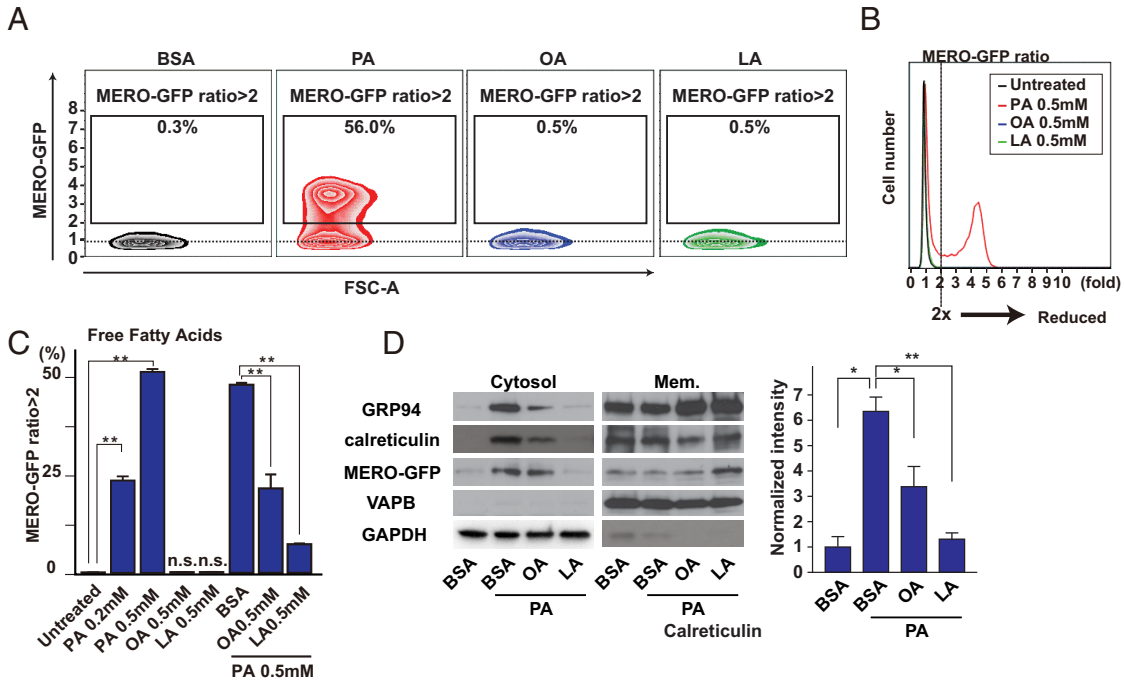

Figure 3. A, Flow cytometric analysis of INS1-MERO-GFP cells treated with BSA, 0.5 mM palmitate (PA), 0.5 mM oleate (OA), or 0.5 mM linoleate (LA) (n = 3). B, Histogram of INS1-MERO-GFP cells treated with 0.5 mM palmitate (PA), 0.5 mM oleate (OA), 0.5 mM linoleate (LA), or untreated. For each analysis, approximately 100 000 cells were analyzed. C, Rate of INS1-MERO-GFP cells treated with indicated free fatty acid. For each analysis, approximately 100 000 cells were analyzed (n = 3). Error bars show SD. *, $P < .05$; **, $P < .01$. D, Immunoblot analysis of cytosol and membrane fractions from INS-1 832/13 cells treated with BSA, 0.5 mM PA and BSA, 0.5 mM PA and 0.5 mM of OA, or 0.5 mM PA and 0.5 mM LA for 24 hours. Right panel shows quantification of cytosolic calreticulin from three independent experiments. *, $P < .05$; **, $P < .01$. Error bars show SD. Each experiment was repeated at least three times independently. Vesicle-associated membrane-associated protein B (VAPB) as a membrane marker.

with the ratio less than 2 (Figure 4B). Because the ER stress response triggers apoptotic signaling in response to intolerable ER stress, we examined whether ER stress-related apoptotic cascades were activated in cells experiencing the ER membrane permeabilization (32). Quantitative PCR analysis showed that ER stress markers, BiP and spliced XBP1, as well as proapoptotic genes in the ER stress response, including Chop and Puma, were significantly up-regulated in cells undergoing the ER membrane permeabilization (Figure 4C) (33–35). Collectively these results indicate that the loss of ER membrane integrity induces ER stress.

We next asked whether the cells harboring an MERO-GFP ratio greater than 2 were susceptible to apoptosis and performed the dual live-cell imaging of MERO-GFP and PI in INS1-MERO-GFP cells treated with palmitate. Both the MERO-GFP ratio and the intensity of PI staining in these cells were measured every 20 minutes. We found that cells harboring highly reduced MERO-GFP eventually underwent cell death (Figure 4D and Supplemental Movie 1). MERO-GFP leaked to the cytosol in dying cells was eventually oxidized (Figure 4D and Supplemental Figure 4).

Discussion

By using mammalian ER-targeted roGFP (MERO-GFP), we have established a method for evaluating the ER membrane integrity in palmitate-treated β-cells at the single-cell level. Palmitate impairs ER membrane integrity, resulting in the leakage of MERO-GFP to the cytosol. The MERO-GFP distributed to the cytosol is immediately reduced, and the ratio between reduced and oxidized MERO-GFP significantly increases upon the leakage. The change in the MERO-GFP ratio can be monitored at the single-cell level in real time. Our method provides new insights into how palmitate induces ER stress and β-cell death in real time, which can be used to develop a novel therapy for protecting β-cells from free fatty acids in diabetes.

Previous studies have shown that palmitate and saturated fatty acids impair ER membrane integrity, leading to apoptosis (15, 17, 26, 36–38). Despite the underlying importance of ER membrane permeabilization in disease states, the mechanisms of loss of ER membrane integrity are still not clear due to methodological limitations. Thus, there is an urgent need to accurately monitor ER mem-

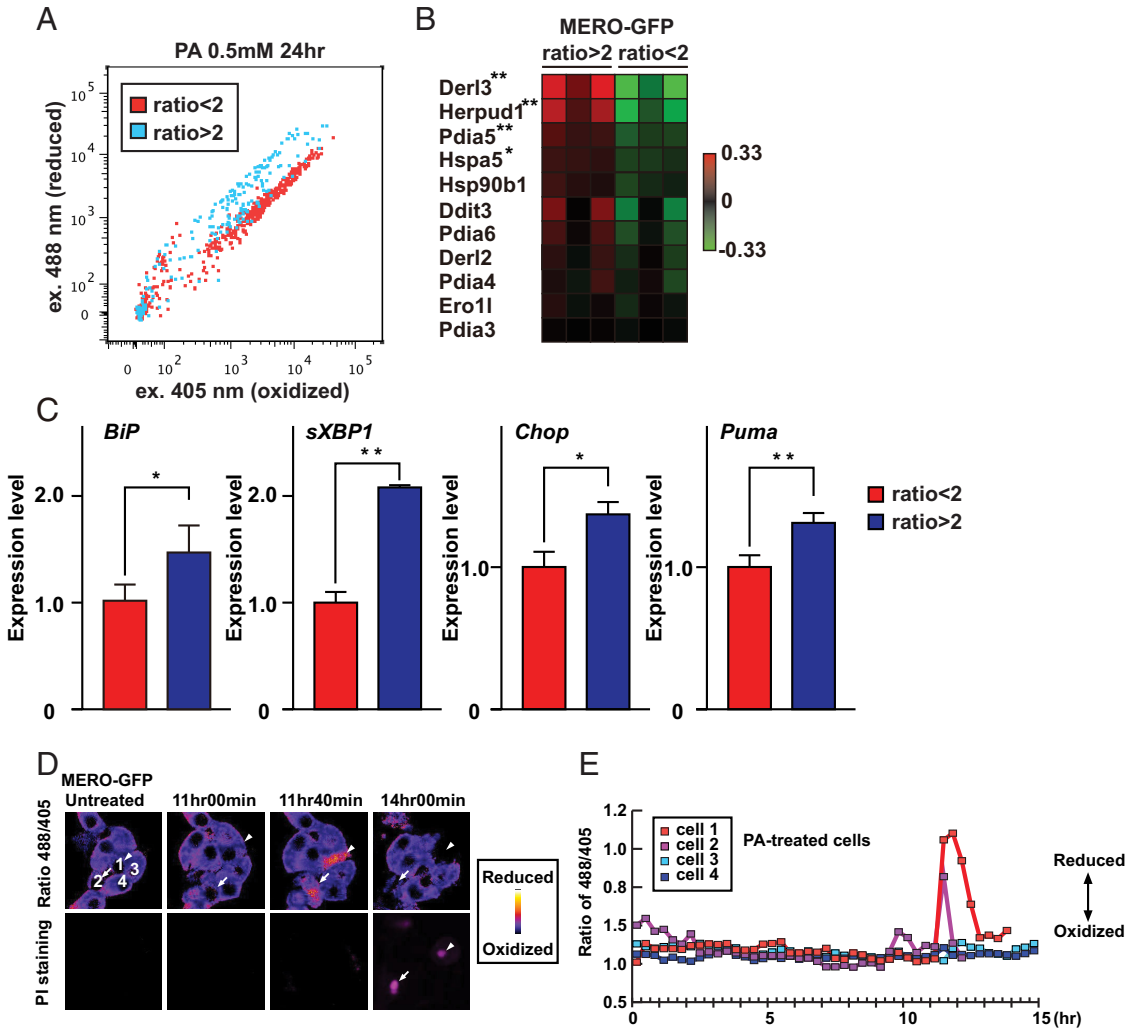

Figure 4. A, A flow cytometric analysis of sorted INS1-MERO-GFP cells treated with 0.5 mM PA for 24 hours. The y-axis shows the signal from excitation 488 nm, and the x-axis indicates the signal from excitation 405 nm. Three samples from each group were sorted. B, Heat map of ER stress-related genes analyzed by microarrays of INS-1 832/13 cells treated with 0.5 mM PA for 24 hours and sorted by the MERO-GFP ratio (n = 3). C, Expression levels of BiP, spliced XBP1 (sXBP1), Chop, and Puma in INS-1 832/13 cells treated with 0.5 mM PA for 24 hours and sorted by the MERO-GFP ratio. Three samples from each group were sorted. The expression levels of target genes were normalized to the one of β-actin. *, $P < .05$; **, $P < .01$. D, Time-lapse ratio imaging of INS1-MERO-GFP cells treated with palmitate (PA; 0.4 mM) for indicated times. The arrowhead (cell number 1) and white arrow (cell number 2) indicate two cells becoming PI positive at 14 hours 00 minutes. E, The MERO-GFP ratio of each cell shown in panel D at the indicated times. Each experiment was repeated at least three times independently.

brane integrity in real time, and this has been successfully accomplished in this study.

The lumen of the ER maintains an oxidative environment with high concentrations of calcium, which is optimized for efficient protein folding. Using the method described in this article, we can potentially identify environmental and pathophysiological factors that disrupt the oxidative environment in the ER. In addition, a flow cytometic analysis and time-lapse imaging identified a previously uncharacterized population of cells generated by palmitate treatment. These cells were isolated by the FACS and characterized. We found that genes involved in ER stress, especially proapoptotic ER stress genes including Chop and Puma, were up-regulated in this cell population undergoing ER membrane permeabilization as compared with a cell population not experiencing it (Figure 4, A–C) (35, 39). We therefore conclude that pancreatic β-cells harboring compromised ER membrane integrity by palmitate undergo cell death due to intolerable ER stress.

Palmitate treatment increased the incorporation of saturated fatty acid into the ER membrane in β-cells, leading to the ER membrane permeabilization and leakage of ER contents to the cytosol (Figures 1 and 3 and Supplemental Figure 1) (20). The mechanisms by which palmitate impairs the ER membrane integrity remain undetermined. The results shown above and a report from others indicate that canonical ER stress inducers, such as tunicamy-

cin, induce ER membrane permeabilization in a Bax/Bak-dependent manner (Supplemental Figure 3B) (16). However, palmitate-mediated ER membrane permeabilization is not mediated by Bax and Bak (Supplemental Figure 3B). One possible mechanism is that palmitate reduces the fluidity of the ER, resulting in the stiff and fragile ER membrane (22).

It is noteworthy that unsaturated fatty acids, such as oleate and linoleate, could prevent ER membrane permeabilization mediated by palmitate (Figure 3, C and D). It has been reported oleate protects pancreatic β-cells from palmitate-mediated β-cell death by suppressing ER stress (40). It is possible that unsaturated fatty acids prevent excess incorporation of palmitate into lipid species and protects the ER membrane from palmitate, which in turn suppresses ER stress.

We have shown here a method for evaluating the ER membrane integrity in palmitate-treated β-cells at the single-cell level. Our method based on ER-targeted roGFP provides new insights into the mechanisms of cell death mediated by compromised ER membrane integrity, which can be targeted to develop novel therapeutic modalities for ER diseases, including β-cell death in diabetes, neurodegeneration, and Wolfram syndrome, a prototype of human ER disease (41, 42).

Acknowledgments

We thank Dr Paul Furcinitti, Dr Lara Strittmatter, Dr Fong Fu Hsu, Mrs Cris Brown, and Mrs Mai Kanekura for technical support.

Address all correspondence and requests for reprints to: Fumihiko Urano, MD, PhD, Department of Medicine, Washington University School of Medicine, 660 South Euclid, Campus Box 8127, St Louis, MO 63110. E-mail: urano@dom.wustl.edu.

K.K. was partly supported by fellowships from the Japan Society for the Promotion of Science and the Uehara Memorial Foundation. F.U. is supported by Grants DK067493 and DK020579 from the National Institutes of Health, Juvenile Diabetes Research Foundation Grant 17-2013-512, American Diabetes Association Grant 1-12-CT-61, the Team Alejandro, the Team Ian, the Ellie White Foundation for Rare Genetic Disorders, and the Jack and J. T. Snow Scientific Research Foundation.

Disclosure Summary: F.U. has received research support from Ono Pharmaceutical CO., LTD. and Amarantus BioScience Holdings, INC. K.K., J.O., T.H., and L.Z. have nothing to declare.

References

1. **Rossini AA, Greiner DL.** Diabetes research in jeopardy: the extinction of clinical diabetes researchers. *Ann NY Acad Sci*. 2007;1103:33–44.
2. **Butler AE, Janson J, Bonner-Weir S, Ritzel R, Rizza RA, Butler PC.** β-Cell deficit and increased β-cell apoptosis in humans with type 2 diabetes. *Diabetes*. 2003;52:102–110.
3. **Donath MY, Halban PA.** Decreased β-cell mass in diabetes: significance, mechanisms and therapeutic implications. *Diabetologia*. 2004;47:581–589.
4. **Karaskov E, Scott C, Zhang L, Teodoro T, Ravazzola M, Volchuk A.** Chronic palmitate but not oleate exposure induces endoplasmic reticulum stress, which may contribute to INS-1 pancreatic β-cell apoptosis. *Endocrinology*. 2006;147:3398–3407.
5. **Kharroubi I, Ladriere L, Cardozo AK, Dogusan Z, Cnop M, Eizirik DL.** Free fatty acids and cytokines induce pancreatic β-cell apoptosis by different mechanisms: role of nuclear factor-κB and endoplasmic reticulum stress. *Endocrinology*. 2004;145:5087–5096.
6. **Zhou YP, Grill VE.** Long-term exposure of rat pancreatic islets to fatty acids inhibits glucose-induced insulin secretion and biosynthesis through a glucose fatty acid cycle. *J Clin Invest*. 1994;93:870–876.
7. **Mason TM, Goh T, Tchipashvili V, et al.** Prolonged elevation of plasma free fatty acids desensitizes the insulin secretory response to glucose in vivo in rats. *Diabetes*. 1999;48:524–530.
8. **Ritz-Laser B, Meda P, Constant I, et al.** Glucose-induced preproinsulin gene expression is inhibited by the free fatty acid palmitate. *Endocrinology*. 1999;140:4005–4014.
9. **Cnop M.** Fatty acids and glucolipotoxicity in the pathogenesis of type 2 diabetes. *Biochem Soc Trans*. 2008;36:348–352.
10. **Cnop M, Igoillo-Esteve M, Cunha DA, Ladriere L, Eizirik DL.** An update on lipotoxic endoplasmic reticulum stress in pancreatic β-cells. *Biochem Soc Trans*. 2008;36:909–915.
11. **Shimabukuro M, Zhou YT, Levi M, Unger RH.** Fatty acid-induced β cell apoptosis: a link between obesity and diabetes. *Proc Natl Acad Sci USA*. 1998;95:2498–2502.
12. **Jeffrey KD, Alejandro EU, Luciani DS, et al.** Carboxypeptidase E mediates palmitate-induced β-cell ER stress and apoptosis. *Proc Natl Acad Sci USA*. 2008;105:8452–8457.
13. **Walter P, Ron D.** The unfolded protein response: from stress pathway to homeostatic regulation. *Science*. 2011;334:1081–1086.
14. **Eizirik DL, Cardozo AK, Cnop M.** The role for endoplasmic reticulum stress in diabetes mellitus. *Endocr Rev*. 2008;29:42–61.
15. **Borradaile NM, Han X, Harp JD, Gale SE, Ory DS, Schaffer JE.** Disruption of endoplasmic reticulum structure and integrity in lipotoxic cell death. *J Lipid Res*. 2006;47:2726–2737.
16. **Wang X, Olberding KE, White C, Li C.** Bcl-2 proteins regulate ER membrane permeability to luminal proteins during ER stress-induced apoptosis. *Cell Death Differ*. 2011;18:38–47.
17. **Diakogiannaki E, Welters HJ, Morgan NG.** Differential regulation of the endoplasmic reticulum stress response in pancreatic β-cells exposed to long-chain saturated and monounsaturated fatty acids. *J Endocrinol*. 2008;197:553–563.
18. **Rainey-Barger EK, Magnuson B, Tsai B.** A chaperone-activated nonenveloped virus perforates the physiologically relevant endoplasmic reticulum membrane. *J Virol*. 2007;81:12996–13004.
19. **Choi SE, Lee SM, Lee YJ, et al.** Protective role of autophagy in palmitate-induced INS-1 β-cell death. *Endocrinology*. 2009;150:126–134.
20. **Fu S, Yang L, Li P, et al.** Aberrant lipid metabolism disrupts calcium homeostasis causing liver endoplasmic reticulum stress in obesity. *Nature*. 2011;473:528–531.
21. **Rintoul DA, Sklar LA, Simoni RD.** Membrane lipid modification of Chinese hamster ovary cells. Thermal properties of membrane phospholipids. *J Biol Chem*. 1978;253:7447–7452.
22. **Spector AA, Yorek MA.** Membrane lipid composition and cellular function. *J Lipid Res*. 1985;26:1015–1035.
23. **Weijers RN.** Lipid composition of cell membranes and its relevance in type 2 diabetes mellitus. *Curr Diabetes Rev*. 2012;8:390–400.
24. **Hitomi J, Katayama T, Taniguchi M, Honda A, Imaizumi K, Tohyama M.** Apoptosis induced by endoplasmic reticulum stress de-

pends on activation of caspase-3 via caspase-12. *Neurosci Lett*. 2004;357:127–130.
25. **Dooley CT, Dore TM, Hanson GT, Jackson WC, Remington SJ, Tsien RY.** Imaging dynamic redox changes in mammalian cells with green fluorescent protein indicators. *J Biol Chem*. 2004;279: 22284–22293.
26. **Martino L, Masini M, Novelli M, et al.** Palmitate activates autophagy in INS-1E β-cells and in isolated rat and human pancreatic islets. *PLoS One*. 2012;7:e36188.
27. **Hanson GT, Aggeler R, Oglesbee D, et al.** Investigating mitochondrial redox potential with redox-sensitive green fluorescent protein indicators. *J Biol Chem*. 2004;279:13044–13053.
28. **Kanekura K, Ishigaki S, Merksamer PI, Papa FR, Urano F.** Establishment of a system for monitoring endoplasmic reticulum redox state in mammalian cells. *Lab Invest*. 2013;93:1254–1258.
29. **Kim JE, Ahn MW, Baek SH, et al.** AMPK activator, AICAR, inhibits palmitate-induced apoptosis in osteoblast. *Bone*. 2008;43:394–404.
30. **El-Assaad W, Buteau J, Peyot ML, et al.** Saturated fatty acids synergize with elevated glucose to cause pancreatic β-cell death. *Endocrinology*. 2003;144:4154–4163.
31. **Hara T, Mahadevan J, Kanekura K, Hara M, Lu S, Urano F.** Calcium efflux from the endoplasmic reticulum leads to β-cell death. *Endocrinology*. 2014;155:758–768.
32. **Oslowski CM, Urano F.** The binary switch that controls the life and death decisions of ER stressed β cells. *Curr Opin Cell Biol*. 2011; 23:207–215.
33. **Tabas I, Ron D.** Integrating the mechanisms of apoptosis induced by endoplasmic reticulum stress. *Nat Cell Biol*. 2011;13:184–190.
34. **Reimertz C, Kogel D, Rami A, Chittenden T, Prehn JH.** Gene expression during ER stress-induced apoptosis in neurons: induction of the BH3-only protein Bbc3/PUMA and activation of the mitochondrial apoptosis pathway. *J Cell Biol*. 2003;162:587–597.
35. **Gurzov EN, Germano CM, Cunha DA, et al.** p53 up-regulated modulator of apoptosis (PUMA) activation contributes to pancreatic β-cell apoptosis induced by proinflammatory cytokines and endoplasmic reticulum stress. *J Biol Chem*. 2010;285:19910–19920.
36. **Maedler K, Spinas GA, Dyntar D, Moritz W, Kaiser N, Donath MY.** Distinct effects of saturated and monounsaturated fatty acids on β-cell turnover and function. *Diabetes*. 2001;50:69–76.
37. **Maedler K, Oberholzer J, Bucher P, Spinas GA, Donath MY.** Monounsaturated fatty acids prevent the deleterious effects of palmitate and high glucose on human pancreatic β-cell turnover and function. *Diabetes*. 2003;52:726–733.
38. **Cnop M, Hannaert JC, Hoorens A, Eizirik DL, Pipeleers DG.** Inverse relationship between cytotoxicity of free fatty acids in pancreatic islet cells and cellular triglyceride accumulation. *Diabetes*. 2001;50:1771–1777.
39. **Song B, Scheuner D, Ron D, Pennathur S, Kaufman RJ.** Chop deletion reduces oxidative stress, improves β cell function, and promotes cell survival in multiple mouse models of diabetes. *J Clin Invest*. 2008;118:3378–3389.
40. **Sommerweiss D, Gorski T, Richter S, Garten A, Kiess W.** Oleate rescues INS-1E β-cells from palmitate-induced apoptosis by preventing activation of the unfolded protein response. *Biochem Biophys Res Commun*. 2013;441:770–776.
41. **Fonseca SG, Fukuma M, Lipson KL, et al.** WFS1 is a novel component of the unfolded protein response and maintains homeostasis of the endoplasmic reticulum in pancreatic β-cells. *J Biol Chem*. 2005; 280:39609–39615.
42. **Shang L, Hua H, Foo K, et al.** β-Cell dysfunction due to increased ER stress in a stem cell model of Wolfram syndrome. *Diabetes*. 2014;63:923–933.